

Excitonic Photoluminescence in Semiconductor Quantum Wells: Plasma versus Excitons

S. Chatterjee, C. Ell, S. Mosor, G. Khitrova, and H. M. Gibbs

Optical Sciences Center, The University of Arizona, Tucson, Arizona 85721-0094

W. Hoyer, M. Kira, and S. W. Koch

*Department of Physics and Materials Sciences Center,
Philipps-University Marburg, Renthof 5, 35032 Marburg, Germany*

J. P. Prineas

Department of Physics and Astronomy, University Iowa, Iowa City, Iowa

H. Stolz

*Department of Physics, University of Rostock,
Universitätsplatz 3, D-18051, Rostock, Germany*

(Dated: June 20, 2018)

Abstract

Time-resolved photoluminescence spectra after nonresonant excitation show a distinct 1s resonance, independent of the existence of bound excitons. A microscopic analysis identifies excitonic and electron-hole plasma contributions. For low temperatures and low densities the excitonic emission is extremely sensitive to even minute optically active exciton populations making it possible to extract a phase diagram for incoherent excitonic populations.

PACS numbers: 71.35.-y, 42.50.-p, 78.70.-g

For a long time, photoluminescence (PL) at the spectral position of the 1s exciton resonance has been considered as evidence for the existence of excitons. The rise of the 1s PL after nonresonant excitation of a semiconductor was interpreted as buildup of an excitonic population [1, 2, 3, 4, 5, 6], and the PL decay was used to describe exciton recombination [7, 8]. However, recently a microscopic theory predicted that PL at the 1s resonance can also originate from correlated plasma emission [9]. Accordingly, PL at the spectral position of the 1s resonance would not prove the existence of excitons, and previous interpretations may be in question. Indeed, in nonresonantly excited time resolved PL measurements the 1s resonance is developed on a sub-ps timescale at 100 K [10], much faster than any expected exciton formation time.

Information about exciton formation can be gained by performing THz experiments [11]. However, currently the THz results are inconclusive: Kaindl et al. [12] observed the buildup of the induced absorption corresponding to the excitonic 1s to 2p transition showing excitonic populations with formation times on a rather slow timescale of 100's of ps to ns. They claim to observe a nearly completely excitonic system 1 ns after excitation, while Chari et al. [13] only plasma contributions. Also, THz absorption is sensitive to both dark and bright excitons, and cannot answer if and how excitonic populations influence the PL. Here we address the following questions. *Is the 1s PL ever dominated by plasma emission? If so, is it always dominated by plasma emission, i.e. what can we learn about excitonic populations from the 1s PL and nonlinear absorption?*

After ps continuum excitation, time resolved PL and corresponding probe absorption measurements are performed under identical conditions on a ns timescale. The sample (DBR42) consists of 20 MBE-grown 8 nm $\text{In}_{0.06}\text{Ga}_{0.94}\text{As}$ quantum wells with 130 nm GaAs barriers; both sides are anti-reflection coated. This indium concentration places the 1s exciton resonance at 1.471 eV at 4 K, avoiding absorption in the bulk GaAs substrate that leads to impurity emission at 1.492 eV from unintentional carbon in the substrate. The results, checked on several other samples including a sample grown in a different MBE system, are insensitive to exciton linewidths or to interfacial or alloy disorder. Single-quantum-well data were noisier but exhibited a similar behavior, excluding significant radiative coupling effects. We excite nonresonantly 13.2 meV above the 1s resonance, into the heavy-hole continuum but below the light-hole resonance. The laser pulses are generated by a Ti:sapphire oscillator emitting 100 fs pulses at 80 MHz. Because of the long PL lifetimes, we use a pulse picker

to reduce the repetition rate to 2 MHz and sweep slowly the Hamamatsu streak camera, decreasing the PL time resolution to 90 ps. For spectrally selective excitation, a tunable 3 ps pulse is generated in a pulse shaper. The pump spot is focussed to $60\ \mu\text{m}$ diameter, three times larger than the probe spot. Both absorption and PL are collected in transmission geometry and spectrally resolved with identical grating monochromators with a spectral resolution of $0.8\ \text{meV}$ [14]. The probe absorption is detected with a liquid nitrogen cooled Si charge-coupled device. The carrier densities at different time delays are estimated from a calibration curve showing the peak height of the nonlinear absorption at 10 ps versus the initial carrier density.

Figure 1 displays measured PL spectra 1 ns after nonresonant excitation for three different densities (solid). All PL spectra exhibit a distinct peak at the 1s exciton resonance ($0\ \text{meV}$). The second peak $6.5\ \text{meV}$ above is due to emission at the 2s resonance; the energetic separation of the resonances yields an $8\ \text{meV}$ binding energy. The continuum PL exhibits an exponential fall-off towards higher energies, from which a carrier temperature is extracted via the Boltzmann factor $\exp(-\Delta E/k_B T)$ by a least squares fit. In order to get a small standard deviation for the temperature values, it is necessary to detect several meV of continuum emission; this requires four to five orders of magnitude dynamic range.

Carrier temperatures extracted from the spectra shown in Fig. 1 are density dependent and vary from $13.5\ \text{K}$ at the lowest density to $20.7\ \text{K}$ at the highest density. Even at later times, they never reach the lattice value of $4\ \text{K}$ [15, 16, 17]; the lowest temperature measured was $10.5 \pm 0.5\ \text{K}$ (2.8 ns after excitation for an initial carrier density of $n_{\text{eh}} = 2.9 \times 10^8\ \text{cm}^{-2}$). For a lattice temperature of $50\ \text{K}$, our measurements show identical lattice and carrier temperatures after $0.1\ \text{ns}$.

To compare many spectra as a function of density and temperature, it is convenient to define a single parameter β to characterize each spectrum. In thermodynamic equilibrium, one expects the PL to be proportional to the absorption coefficient α times a Bose distribution function $g(\hbar\omega - \mu) = 1/(\exp^{(\hbar\omega - \mu)/k_B T} - 1)$, i.e. $I_{\text{PL}}^{\text{eq}}(\hbar\omega) \propto g(\hbar\omega - \mu)\alpha(\hbar\omega)$ where μ is the joint chemical potential of the electron-hole plasma; this is known as the Kubo-Martin-Schwinger (KMS) relation [18]. We then define $\beta = I_{\text{PL}}(1s)/I_{\text{PL}}^{\text{eq}}(1s)$ as in [17]. $I_{\text{PL}}^{\text{eq}}(\hbar\omega)$ is found by multiplying the measured nonlinear α by a Boltzmann factor to approximate the Bose function, using the temperature extracted from the measured continuum emission and normalizing it to agree with the measured continuum PL; see dashed lines in Fig. 1. Thus

β quantifies how the 1s emission of a given spectrum differs from that expected from the measured absorption assuming validity of the KMS relation.

Figure 2 displays the density dependence of β for lattice temperatures of 50 K (top) and 4 K (bottom). We find significant deviation from $\beta = 1$ for all densities, temperatures, and times, implying that KMS is never valid for the configurations studied here. The 50 K result varies only slightly across the investigated density range. For the lower lattice temperature, we find pronounced deviations from the thermal equilibrium result particularly for low densities. For elevated densities, β exhibits an increase to values of around 0.5.

In order to analyze the experimental observations, we apply our microscopic theory that treats Coulomb interacting electrons and holes, phonons and a quantized light field. The details of the theory can be found in previous publications [9, 19]. This theory, evaluated at the level of a Hartree-Fock approximation first predicted luminescence at the exciton energy without exciton populations [9]. Meanwhile we have extended the analysis to include also electron-hole correlations and bound excitons. We use an adiabatic treatment of the photon-assisted polarizations such that the steady-state luminescence can be obtained from

$$I_{\text{PL}}(\omega) = \frac{|d_{\text{cv}}^2| \omega}{\varepsilon_{\text{bg}}} \text{Im} \left[\sum_{\nu} \frac{\phi_{\nu}^r(r=0)}{E_{\nu} - \hbar\omega - i\gamma_{\nu}} \sum_{k,k'} (\phi_{\nu}^l(k))^* \langle a_{c,k'}^{\dagger} a_{c,k} a_{v,k'} a_{v,k}^{\dagger} \rangle \right], \quad (1)$$

where $a_{\lambda,k}^{\dagger}$ creates an electron in band $\lambda = c, v$ in quantum state k . The prefactor in Eq. (1) is determined by the square of the dipole matrix element $|d_{\text{cv}}|^2$ and the background dielectric constant ε_{bg} [20]. Equation (1) is reminiscent of the famous Elliott formula for bandgap absorption [21]; it contains a sum over excitonic states, and the resonances of the denominator show that the PL peaks at the same excitonic energies as the absorption. In contrast to the absorption, however, the strength of the PL is not only determined by the exciton wavefunctions but also by the source term $\sum_{k,k'} (\phi_{\nu}^l(k))^* \langle a_{c,k'}^{\dagger} a_{c,k} a_{v,k'} a_{v,k}^{\dagger} \rangle$. This source contains a plasma contribution $[\phi_{\nu}^r(r=0)]^* \sum_k |\phi_{\nu}^l(k)|^2 f_k^e f_k^h$ which is always present as soon as electrons and holes are excited. Moreover, the source term can also describe incoherent bound excitonic correlations N_X which may or may not be in the system.

The theory-experiment comparison over the experimentally relevant density regime requires the proper description of the microscopic Coulomb scattering which is different for the correlation terms in comparison to the scattering of the photon-assisted polarizations.

The exciton basis used in the calculations is not the usual low-density one, instead, left- and right handed basis functions $\phi^{l/r}$ have to be taken into account. Furthermore, not only the eigenenergies $E_\nu(\omega)$ but also the broadenings $\gamma_\nu(\omega)$ depend on the excitonic index and the emission frequency. Separating the excitonic and plasma populations we evaluate our theory and determine the β factor. Here, the respective excitonic and plasma populations are treated as input to the theory, and a fit to the measured PL spectra is obtained by varying the optically active ($q = 0$) 1s-exciton population. Thus, this formulation of the theory allows us to formally distinguish between electron-hole plasma and bound excitons as different possible sources to excitonic PL.

Computed spectra are shown in Fig. 3. There the pure plasma PL (dotted line) is compared to the KMS result (dashed line) obtained from the computed absorption. The corresponding β factors are plotted as dotted lines in Fig. 2. At 50 K, the bare plasma emission shows good agreement with the experimental β 's over almost the whole density range. Even for 4 K, the highest density results agree. Note that the exciton absorption is still very pronounced with the peak reduced by only 25%. This answers our first question: *the 1s PL can be dominated by plasma emission, and the spectra explained by a pure plasma theory; this is the case at high temperatures and even at low temperatures for higher densities.*

Figure 2 also shows that at 4 K and low to intermediate densities, the pure plasma calculation underestimates β . We attribute the stronger measured 1s emission to the presence of incoherent bound 1s-exciton populations N_X and test this hypothesis by adding optically active $q = 0$ excitons in the theory. Fig. 3 shows that this addition strongly enhances the 1s PL. Since the plasma contribution changes quadratically with the carrier density, even minute exciton fractions result in a strong enhancement of the 1s resonance. The addition of excitons allows us to obtain an excellent theory-experiment agreement for β for all densities; see solid lines in Fig. 2. The inset shows the bright excitons necessary for that agreement.

When the 1s-exciton distribution is expressed as $N_X(q) = N_X(q = 0) F(q)$ with $F(q = 0) = 1$, only the $q = 0$ value can be deduced from the theory-experiment comparison. Thus it is impossible to determine the total number of excitons from PL measurements. If we assume a thermal distribution at 4 K, the largest value in the inset of Fig. 2 corresponds to a total exciton fraction of 4%. However, if significant hole burning [11, 22] in the 1s distribution around $q = 0$ is present, this number could be much larger. This answers our second question: *at low temperatures and for low and intermediate densities, the 1s PL*

is dominated by the recombination of excitons, even though the density of optically active excitons may be only a small fraction of the plasma density. Consequently, depending upon temperature and density, excitonic PL can be almost entirely from the plasma or almost entirely from excitons.

Even though our PL studies cannot determine the total exciton number or the detailed exciton distribution function, our results clearly show an increased importance of excitons at lower lattice temperatures and intermediate densities. This observation is in qualitative agreement with exciton formation studies in quantum wires [19]. Due to kinetic arguments, exciton formation after nonresonant excitation should be most efficient at intermediate densities. At low densities the probability for electron-hole collisions is too small, whereas at higher densities exciton binding is hampered by phase space effects and screening of the attractive Coulomb interaction.

We can further investigate the low-density behavior by studying the temporal evolution of β shown in Fig. 4. Because the experiment is pulsed, the carrier density decays with time. While β does not vary significantly in the strong excitation regime, implying that a quasi-steady-state has been reached, it decays monotonically at lower densities. The inset, like Fig. 2 for low densities, contains β values at several time delays all ≥ 1 ns to exclude cooling effects [15]. The functional behavior follows an interpolated curve through the 1 ns values (squares). Here the decay of β and the corresponding exciton fraction are thus fully parameterized by the density decay. This shows that β depends not upon past history, but only upon the momentary carrier density and temperature, as needed for comparison with a quasi-steady-state theory.

In conclusion, by carefully mapping out the parameter space of carrier density and lattice temperature, we have identified conditions under which the PL emission at the 1s resonance after nonresonant excitation into the continuum is dominated by the plasma or by an incoherent excitonic population. We observe that the appearance of the 1s-exciton resonance in PL is ubiquitous, independent of the existence of bound excitons and that the KMS relation is never fulfilled. In particular, the 1s emission is always weaker than that predicted by KMS. Under suitable conditions excitons may form after nonresonant excitation, and we identify a regime of low temperature and intermediate density as most favorable.

Acknowledgments

The work is supported in Tucson by NSF (AMOP), AFOSR (DURINT), and COEDIP and in Marburg by the Deutsche Forschungsgemeinschaft through the Quantum Optics in Semiconductors Research Group, by the Humboldt Foundation and the Max-Planck Society through the Max-Planck Research prize, and by the Optodynamics Center of the Philipps-Universität Marburg.

- [1] J. Kusano et al., Phys. Rev. B **40**, 1685 (1989).
- [2] T. C. Damen et al., Phys. Rev. B **42**, 7434 (1990).
- [3] R. Eccleston et al., Phys. Rev. B **44**, 1395 (1991).
- [4] P. W. M. Blom et al., Phys. Rev. Lett. **71**, 3878 (1993).
- [5] R. Kumar et al., Phys. Rev. B **54**, 4891 (1996).
- [6] M. Gulia et al., Phys. Rev. B **55**, 16049 (1997).
- [7] J. Feldmann et al., Phys. Rev. Lett. **59**, 2337 (1987).
- [8] B. Deveaud et al., Phys. Rev. Lett. **67**, 2355 (1991).
- [9] M. Kira, F. Jahnke, and S. W. Koch, Phys. Rev. Lett. **81**, 3263 (1998).
- [10] G. R. Hayes and B. Deveaud, Phys. Status Solidi A **190**, 637 (2002).
- [11] M. Kira et al., Phys. Rev. Lett. **87**, 176401 (2001).
- [12] R. A. Kaindl et al., Nature **423**, 734 (2003).
- [13] R. Chari et al., QELS 2003 postdeadline.
- [14] To better utilize the dynamic range of the streak camera a film neutral density filter was placed at the exit plane of the corresponding monochromator reducing the fluence by 40 for all energies < 1.474 eV. The shown data are multiplied by this factor to present them undistorted.
- [15] K. Leo et al., Phys. Rev. B **37**, 7121 (1988).
- [16] H. W. Yoon, D. R. Wake, and J. P. Wolfe, Phys. Rev. B **54**, 2763 (1996).
- [17] R. F. Schnabel et al., Phys. Rev. B **46**, 9873 (1992).
- [18] R. Kubo, J. Phys. Soc. Japan **12**, 570 (1957); P.C. Martin and J. Schwinger, Phys. Rev. **115**, 1342 (1959).

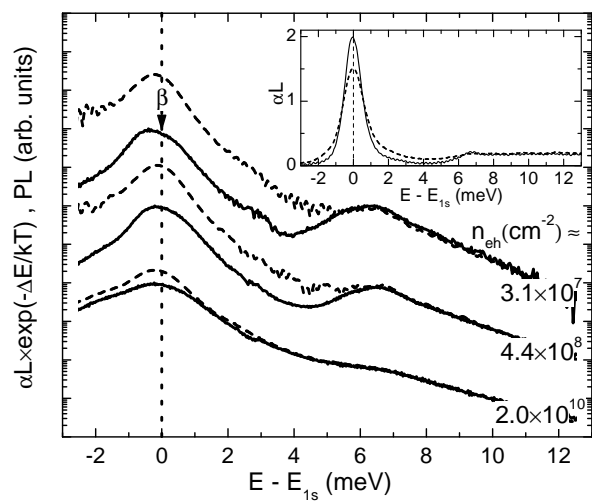
- [19] W. Hoyer, M. Kira and S. W. Koch, Phys. Rev. B **67**, 155113 (2003).
- [20] Our calculations are performed for finite quantum well widths and infinite barrier heights. We adjust the effective well width such that our calculations reproduce the experimentally measured exciton binding energy. $m_h/m_e = 3$ as determined using $k \cdot p$ theory, the other material parameters cancel out of the β calculations.
- [21] R. J. Elliott, Phys. Rev. **108**, 1384 (1957).
- [22] C. Piermarocchi et al., Phys. Rev. B **53**, 15834 (1996).

FIG. 1: Experimental PL spectra (solid) for a lattice temperature of 4 K are compared to the KMS result $I_{\text{PL}}^{\text{eq}}(\hbar\omega)$ (dashed), i.e. the measured nonlinear αL multiplied by the Boltzmann factor. PL is integrated from 0.95 to 1.05 ns after nonresonant excitation, and the densities are for $t = 1$ ns. The corresponding curve pairs are vertically offset by two decades. Inset: Nonlinear absorption spectra for the highest (dashed) and lowest densities (solid).

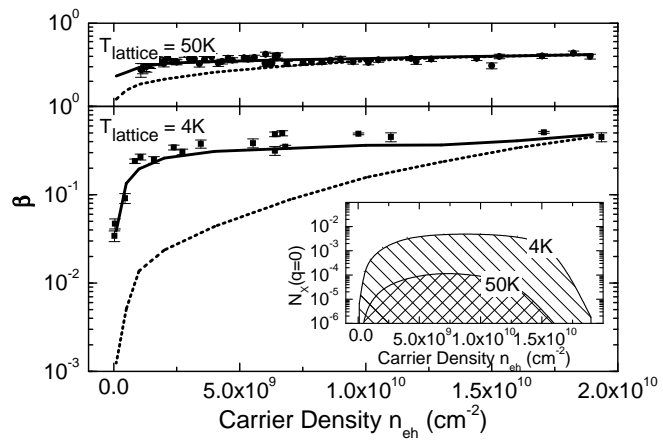
FIG. 2: β versus carrier density. Full squares refer to experimental values taken at 1 ns after nonresonant excitation at a lattice temperature of 4 K. The densities refer to densities at 1 ns. The theoretical values (dotted line) are calculated using the PL formula (1) for a pure e-h plasma with a carrier temperature of 16 ± 2 K. The solid line shows a theoretical fit including a $q = 0$ exciton contribution. Top: same for 50 K lattice temperature and extracted e-h plasma temperature of 50 ± 3 K; the theoretical curves are computed for a carrier temperature of 48 K. Inset: Phase diagram of $q = 0$ excitonic contributions as a function of the carrier density.

FIG. 4: Experimental β values versus time for 4 K lattice temperature. For nonresonant excitation $\beta < 1$, i.e. the 1s emission is less than for thermal equilibrium. The carrier densities (cm^{-2}) at 1 ns are 2.0×10^{10} (dots), 1.1×10^9 (triangles), 4.4×10^8 (diamonds), and 3.1×10^7 (stars). The inset shows the low density part of beta versus carrier density, and an additional set (open circles) with a carrier density of 4.7×10^7 at 1 ns. The data points shown are taken for times ≥ 1 ns.

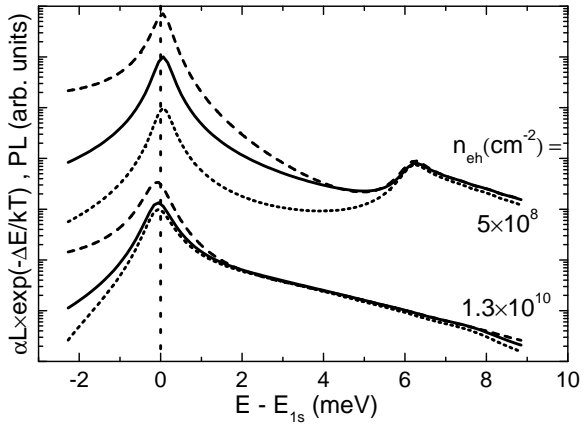
FIG. 3: Theoretical PL spectra for various densities for a carrier temperature of 16 K: pure plasma (dotted) and including excitons (solid). The exciton contributions used are chosen to give agreement with the experimental β as shown in Fig. 2. The KMS result (dashed) is obtained by multiplying the computed nonlinear αL by the Boltzmann factor.



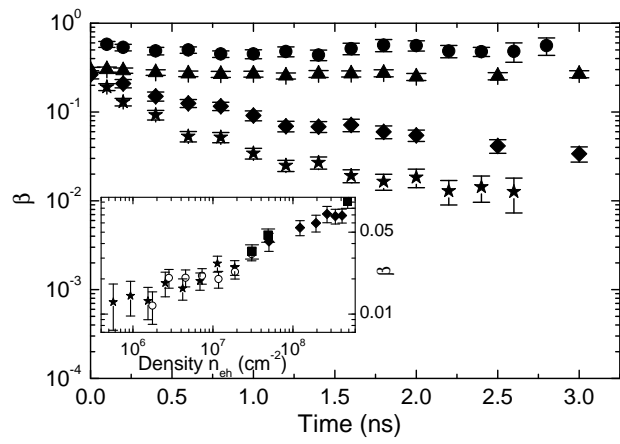
Chatterjee et al., Fig. 1



Chatterjee et al., Fig. 2



Chatterjee et al., Fig. 3



Chatterjee et al., Fig. 4